Breath Patterns as Signals: A Machine Learning-based Molecular Communication Perspective

Sunasheer Bhattacharjee*, Saswati Pal*, Péter Scheepers, and Falko Dressler
School of Electrical Engineering and Computer Science, TU Berlin, Germany
{bhattacharjee,pal,scheepers,dressler}@ccs-labs.org

Abstract

Molecular communication is a core pillar of the Internet of Bio-Nano Things. Exhaled breath, rich in water vapor, offers a viable medium for air-based molecular communication. This paper presents a low-cost, non-invasive approach using a DHT22 sensor to classify breath patterns, namely Eupnea, Bradypnea, and Tachypnea. Humidity and temperature signals from the mouth and nose are processed using machine learning (ML). The model achieves strong classification performance, showing that ML can effectively distinguish breath patterns despite sensor constraints.

CCS Concepts

• **Hardware → Sensors and actuators**; • **Applied computing → Health care information systems**.

Keywords

Biological system, diagnostics, communication system model, machine learning, molecular communication

ACM Reference Format:
Sunasheer Bhattacharjee, Saswati Pal, Péter Scheepers, and Falko Dressler. 2025. Breath Patterns as Signals: A Machine Learning-based Molecular Communication Perspective. In *The 12th Annual ACM International Conference on Nanoscale Computing and Communication (NANOCOM '25), October 23–25, 2025, Chengdu, China.* ACM, New York, NY, USA, 6 pages. https://doi.org/10.1145/3760544.3764127

1 Introduction

The Internet of Bio-Nano Things envisions nanoscale biological and artificial devices communicating via molecular or terahertz signals [1, 11], but its medical use faces challenges like miniaturization and bio-compatibility. As a practical alternative, the Internet of Bio Things leverages biological transmitters (e.g., humans) and engineered receivers via air-based molecular communication (ABMC) [5, 19]. This framework supports non-invasive breath-based monitoring with existing sensing technologies and communication models, thereby bridging molecular communication (MC) theory with real-world health applications.

Exhaled breath contains a complex mix of biomarkers, including gases like carbon dioxide, oxygen, nitrogen, and volatile organic compounds (VOCs) [20], apart from aerosolized particles such as water vapor, dust, and pollen [12]. Together, they reflect the physiological and pathological states of a human body.

This paper presents a low-cost method for classifying Eupnea, Bradypnea, and Tachypnea using a DHT22 humidity and temperature sensor. Even with modest fidelity, temporal humidity and temperature changes reveal key health indicators when processed with supervised machine learning (ML). The single-sensor, wearable-compatible setup bridges theoretical ABMC models with real-world respiratory monitoring.

The key contributions of our work include:

- Application of ABMC for decoding human breath patterns using low-cost humidity and temperature sensing.
- Demonstration of accurate classification of three core respiratory states using supervised ML pipeline based on stacking classifiers, despite the simplicity of the DHT22 sensor.
- A minimalistic and non-invasive framework that links ABMC theory with practical health monitoring applications.

The remainder of this paper is organized as follows: Section 2 reviews related work on ABMC and breath analysis. Section 3 presents the proposed system model, mapping MC components to physiological processes in exhaled breath. Section 4 describes the three investigated respiratory patterns. Section 5 details the hardware setup and data collection methodology. Section 6 introduces the ML-based breath pattern classification model. Section 7 evaluates the performance of the model. Finally, Section 8 concludes the paper and outlines directions for future research.

2 Related Work

ABMC has emerged as a promising approach for health detection and communication. Several studies have explored this potential both in theory and in practice [5, 25].

The concept of MC using chemical or physical carriers has been well established in the literature, particularly through foundational works such as that of Farsad et al. [14]. They demonstrated a table-top MC system using alcohol as a carrier. Although their work pioneers practical MC systems, it focuses primarily on controlled environments and symbolic message transfer, rather than physiological monitoring.

Khalid et al. [16] introduced an approach conceptualizing human breath as a viable information source for communication systems. Their study largely illustrates the idea of using exhaled breath comprising VOCs, water vapor, and pathogenic aerosols as information carriers in an aerosol-based MC framework. However, their work remains largely theoretical and simulation-based, focusing on particle dynamics and spread.

* S. Bhattacharjee and S. Pal contributed equally to this work and are listed as co-first authors alphabetically.

NANOCOM '25, October 23–25, 2025, Chengdu, China

ACM ISBN 979-8-4007-2166-3/2025/10…$15.00
https://doi.org/10.1145/3760544.3764127

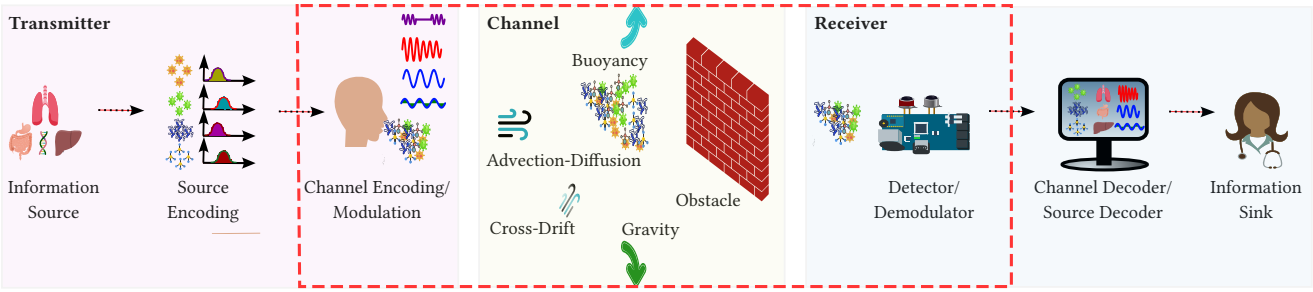

Figure 1: System model for analyzing the exhaled breath from a source via a channel to a sink.

Radogna et al. [23] developed a breath analyzer module integrated into non-invasive ventilation setups for chronic obstructive pulmonary disease monitoring. However, their approach uses multiple sensors in a clinical context, where the system captures exhaled breath data during home-assisted ventilotherapy sessions and transmits them to healthcare providers for continuous evaluation.

Chen et al. [8] proposed a portable electronic nose system based on a graphene-based chemiresistive sensor array for online exhaled breath analysis and non-invasive disease diagnosis. Their approach demonstrates high classification accuracy for respiratory diseases using ML and a specialized gas chamber design. However, their system requires complex circuitry and expensive multi-sensor integration for exhaled breath gas profiling.

As we go beyond these initial works and analyze the limitations, key challenges arise such as reliance on simulation frameworks, controlled experimental setup, or complex, multi-sensor clinical system. This paper addresses these issues by combining ABMC with supervised ML in a single, low-cost DHT22 sensor platform.

3 System Model

In the following, we outline the analogy between the standard communication model and an MC framework for health diagnostics via exhaled breath. Figure 1 maps the transmitter, channel, and receiver to their biological counterparts. The **information source** represents the message origin, corresponding in ABMC to a person's metabolic or health state, such as diabetes, cancer, or infections, along with their location and severity. For example, acetone may indicate diabetic ketoacidosis or a ketogenic diet, highlighting the need to distinguish overlapping sources. Severity (e.g., disease type or stage) offers deeper insights into progression and impact.

In exhaled breath analysis, **source encoding** describes how metabolic processes translate health conditions into measurable biomarkers of disease presence, location, and severity. Metabolic activities generate biochemical signals encoded as discrete biomarkers, e.g., acetone for diabetic ketoacidosis and nitric oxide for asthma-related inflammation. This process compresses complex biological signals into interpretable health data. Redundancy in **channel encoding** arises from repeated biomarker emissions at consistent levels, reducing noise and errors. For example, multiple coughs act as repetition coding to strengthen the signal.

Modulation refers to breath exhalation, where biomarker properties like type, concentration, timing, and spatial distribution [6] encode health status, condition location, and severity. Irregular breath patterns [17, 18] act as modulated signals reflecting physiological or pathological changes.

The **channel** in breath analysis is the ambient air, where biomarker-laden aerosols propagate via diffusion, advection, buoyancy, gravity, and initial drift. External factors like airflow or walls introduce noise that unintentionally affects propagation.

For **demodulation**, sensors extract information from exhaled biomarkers such as VOCs, nitrogen oxides, and CO_2, which reflect metabolic and physiological states. Metal-oxide gas sensors, for example, detect and demodulate these signals based on biomarker type, concentration, and timing. Accurate interpretation relies on onboard computing for signal processing and pattern recognition, often using ML techniques [27].

Channel decoding helps in the extraction of information from exhaled biomarkers that have been affected by noise during transmission. This involves applying error detection and/or correction techniques to compensate for noise and distortions, thus improving the accuracy of the recovered information. **Source decoding** maps the detected and demodulated biomarkers to their associated physiological conditions and anatomical origins. This step involves analyzing raw biomarker data patterns, and then relating them to established health conditions, metabolic abnormalities, or inflammatory processes.

Finally, at the **information sink**, the decoded data represents the individual's physiological and pathological states, supporting personalized medical decisions. However, effective integration requires user training, as new workflows in electronic health record systems can temporarily reduce efficiency [3].

Although the end-to-end system model treats exhaled biomarkers as information carriers originating from the source, our work focuses specifically on the modulation and physical transport of aerosolized water vapor, as highlighted by the red-dashed section in Figure 1. This component directly shapes the signal patterns received for detection and classification.

4 Breath Patterns

In this work, we investigated three distinct respiratory patterns, namely, Eupnea, Bradypnea, and Tachypnea. These patterns not only reflect underlying physiological or pathological states but also influence the dynamics of exhaled signal generation and transmission from the perspective of ABMC.

Eupnea refers to normal, quiet, unlabored breathing that maintains gas exchange under resting metabolic demand. It is typically defined by a respiratory rate (RR) of 12 to 20 breaths per minute

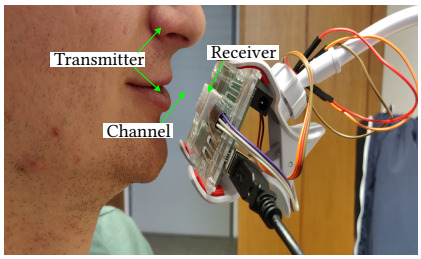

Figure 2: Sensor assembly as used in our experiments. The sensors are positioned close to mouth and nose.

with balanced inspiratory and expiratory phases [17]. Eupnea reflects proper function of respiratory centers in the *medulla* and *pons*, along with healthy pulmonary and neuromuscular systems [26]. It is driven by metabolic needs and regulated by chemoreceptor feedback to arterial blood gases [4]. As a reference pattern in pathological assessment, Eupnea serves as the baseline for signal generation, propagation, and detection in ABMC.

Bradypnea denotes an abnormally slow RR, typically defined as fewer than 12 breaths per minute in adults [17]. Physiological states such as deep sleep, meditation, or yogic breathing may feature Bradypnea without pathological consequence. However, Bradypnea can be symptomatic of serious conditions such as opioid overdose, brainstem injury, and hypothyroidism [2, 7, 13].

Tachypnea is defined as rapid breathing with RR exceeding 20 breaths per minute in adults [17]. Physiologically, it may arise during exercise, anxiety, or emotional arousal, while pathologically it is common in conditions such as pneumonia, pulmonary embolism, sepsis, and diabetic ketoacidosis [24].

5 Hardware Setup and Data Collection

We use a DHT22 sensor with Arduino Uno (digital pin D3) to monitor humidity and temperature variations during Eupnea, Bradypnea, and Tachypnea, sampling data every 2 s. The sensor is mounted on a flexible gooseneck approximately 3 cm from the subject's nose or mouth to capture rapid changes in humidity and temperature in breath, while minimizing ambient interference (cf. Figure 2). Data were collected from three healthy adults (two males, one female, aged 25–35), with non-Eupnea patterns artificially emulated. The DHT22 provides a low-cost, non-invasive way to capture physiological signals linked to different breath patterns.

The channel impulse response was measured at the mouth and nose by averaging 10 trials over short span in order to reduce environmental variability. Using the DHT22 sensor, humidity and temperature during exhalation were recorded and baseline-corrected. As shown in Figure 3, mouth readings are typically higher due to greater exhaled volume, airflow, and heat exchange characteristics.

Humidity and temperature were recorded for Eupnea, Bradypnea, and Tachypnea from both mouth and nose. Each 70 s trial begins with a 10 s resting baseline. Figure 4 presents five representative Eupnea trials recorded from both the mouth and nose, illustrating the temporal trends. Due to sensor response limitations, humidity gradually increases and plateaus, while temperature shows a steady rise, reflecting exhaled thermal patterns.

6 Breath Pattern Classification Model

At the receiver, we classify breath patterns, namely, Eupnea, Bradypnea, and Tachypnea using a proposed ML model trained on time-series humidity and temperature data from the DHT22 sensor. Each breath pattern is treated as a distinct modulation pattern similar to symbol encoding in ABMC systems.

We collected a data set consisting of 645 multivariate time-series recordings of respiratory activity from the mouth (271 samples) and nose (374 samples), labeled as Eupnea, Bradypnea, or Tachypnea. Each trial, saved in a separate file, represents a single breathing session similar to the trials shown in Figure 4. To preserve data integrity and ensure controlled sampling across different breath patterns, we included all trials that matched predefined filename prefixes and grouped them by class. We loaded each trial in a structured format with an identifier and uniformly increasing time index to support time-series analysis. Finally, we numerically encoded the class labels using a predefined label mapping dictionary to ensure consistent representation of target labels. This annotated data set forms the foundation for feature extraction.

The primary goal is to build a robust and interpretable model to distinguish between Eupnea, Bradypnea, and Tachypnea using features extracted from raw time-series data. The model takes multivariate time-series data as input, represented as $\mathbf{X} \in \mathbb{R}^{T \times d}$, where T is the number of time steps and d is the number of sensor outputs (humidity and temperature) for each sample. For each signal, a feature extraction mapping Φ is applied to generate a feature vector $\mathbf{x} = \Phi(\mathbf{X}) \in \mathbb{R}^p$, where p is the number of extracted features. Specifically,

$$\mathbf{x} = \Phi(\mathbf{X}) = \left[\phi_1(\mathbf{X}),\ \phi_2(\mathbf{X}),\ \ldots,\ \phi_p(\mathbf{X})\right], \tag{1}$$

where Φ denotes a set of statistical, temporal, and spectral functions applied to the time-series input $\mathbf{X}$ to extract a p-dimensional feature vector $\mathbf{x} \in \mathbb{R}^p$. Each component $\phi_j(\mathbf{X})$ corresponds to a specific feature such as mean, variance, autocorrelation, entropy, etc. We implement this transformation using the `tsfresh` library [10], which automatically extracts 419 features for mouth samples (180 from humidity, 239 from temperature) and 243 for nose samples (148 from humidity, 95 from temperature). After extracting features, we impute missing values, standardize the feature matrix to ensure uniform scaling, and clean the column names to ensure they follow valid naming conventions.

We design the model pipeline to minimize information leakage, handle class imbalance, and boost performance via ensemble learning. To ensure balanced class representation, stratified sampling is applied when splitting the data. The mouth data set includes 216 training and 55 testing samples, while the nose data set has 299 training and 75 testing samples. For interpretability, we use SHapley Additive exPlanations (SHAP)[1] with a tuned LightGBM classifier to assess feature importance. SHAP provides trial-level insights, identifies non-linear interactions, and highlights weak/redundant features, critical for high-dimensional time-series data. SHAP summary plots and heat maps show model behavior across respiratory classes. To reduce dimensionality, we select the top 20 features ranked by the magnitude of their SHAP values, represented as

$$S = \mathrm{Top}_{20}\left(|\phi_1|,\ |\phi_2|,\ \ldots,\ |\phi_p|\right). \tag{2}$$

[1] https://pypi.org/project/shap/

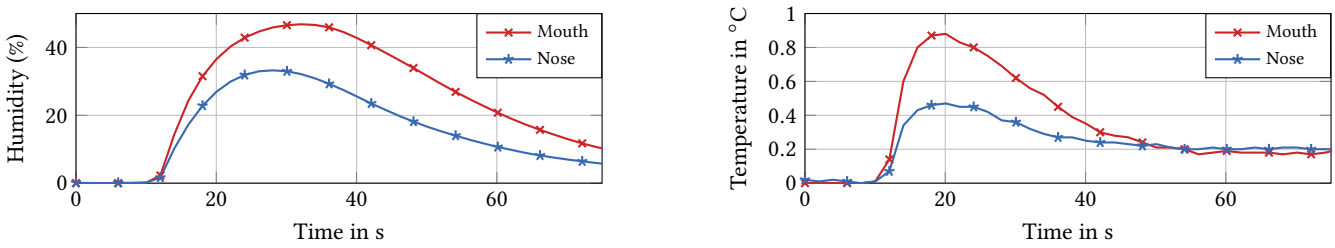

(a) Humidity **(b) Temperature**

Figure 3: Channel impulse response averaged over 10 trials and baseline corrected for both mouth and nose.

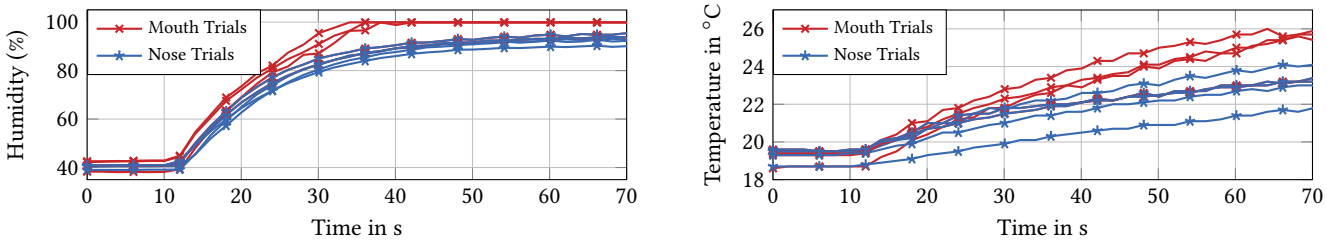

(a) Humidity **(b) Temperature**

Figure 4: Humidity and temperature trends for Eupnea over 5 trials each from mouth and nose.

This results in a compact, efficient, and interpretable feature set used to retrain the model without compromising accuracy.

We use the reduced feature set to construct a stacked ensemble classifier, employing XGBoost [9] and CatBoost [22] as base learners and Random Forest [21] as meta-learner. In this pipeline, the outputs of k base classifiers $h_1, h_2, \ldots, h_k$ (here, $k = 2$) are provided as inputs to a meta-learner, which combines their predictions to produce the final output. For each trial, the subvector $\mathbf{x}_S \subset \mathbf{x}$, containing the SHAP-selected subset of features, is provided as input to both base classifiers. The ensemble prediction is then computed as

$$H(\mathbf{x}_S) = f\left(h_1(\mathbf{x}_S),\ h_2(\mathbf{x}_S)\right), \tag{3}$$

where $\mathbf{x}_S$ is the SHAP-selected feature subset, and f denotes the Random Forest meta-learner. This setup combines base model outputs with SHAP-selected features enhancing model diversity and classification. To address class imbalance, we apply synthetic minority over-sampling technique (SMOTE)[2] to the training data. We train and validate the stacked model using stratified 5-fold cross-validation (CV), ensuring robustness and generalization across different subsets of the data. The final prediction $\hat{y} = H(\mathbf{x}_S)$ is evaluated using CV accuracy, test accuracy, class-wise receiver operating characteristic area under the curve (ROC-AUC) scores, and confusion matrix analysis. The key parameters of the ML model are summarized in Table 1.

Table 1: Summary of most relevant ML parameters.

Component	Parameter	Value / Description
LightGBM Classifier (for SHAP-based feature selection)	n_estimators	300–1000
	learning_rate	0.05
	max_depth	4–6
	subsample	0.8
	colsample_bytree	0.8
	reg_alpha, reg_lambda	0.1–1.0
	Hyperparameter Tuning	GridSearchCV (mouth only)
Data Split	Train-Test Ratio	80% train / 20% test
	Stratification	Yes (to maintain class balance)
Feature Engineering	Selection Method	SHAP-based ranking (top 20)
	Data Balancing	SMOTE (after feature selection)
Ensemble Strategy	Method	StackingClassifier
	Base Models	XGBoost, CatBoost
	Cross-validation	StratifiedKFold (n_splits=5)
Random Forest Meta Classifier	n_estimators	150
	max_depth	3

7 Performance Evaluation

In the following, we present selected results and evaluate the performance of the ML model in classifying breath patterns using mouth and nose data. The model, trained on SHAP-selected features, is assessed using CV and test set metrics to evaluate accuracy [15] and interpretability. All sensor data and the Python code used for model evaluation are publicly available under CC BY and MIT licenses[3].

7.1 Results

Figure 5 summarizes the performance of the ensemble model for the mouth-based data. The learning curve in Figure 5a shows rapid training accuracy saturation close to 100 % with increasing number of training samples, indicating a good fit of the model to the training data. Additionally, the CV accuracy also steadily increases to 93.7 % with increasing number of training samples, indicating the generalizability of the model. The final test accuracy of 94.6 % closely matches CV performance, confirming strong generalization of the model. The narrowing gap between training and CV accuracy

[2]https://imbalanced-learn.org/stable/references/generated/imblearn.over_sampling.SMOTE.html
[3]https://doi.org/10.5281/zenodo.15697086

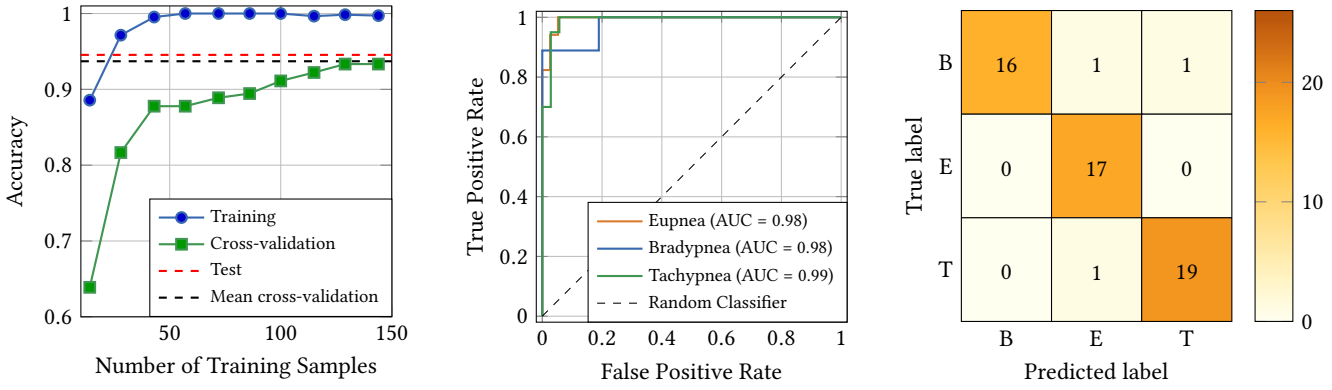

(a) Learning rate **(b) Receiver operating characteristics** **(c) Confusion matrix**

Figure 5: Performance of the ensemble model for the mouth-based data set.

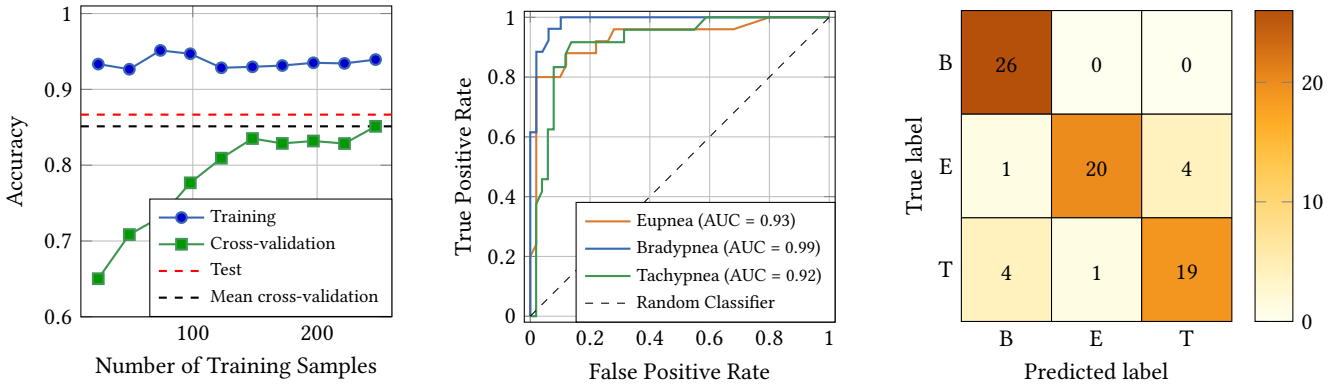

(a) Learning rate **(b) Receiver operating characteristics** **(c) Confusion matrix**

Figure 6: Performance of the ensemble model for the nose-based data set.

further suggests model stability. Figure 5b shows receiver operating characteristic (ROC) curves for Eupnea, Bradypnea, and Tachypnea, with high area under the curve (AUC) values of 0.98 for both Eupnea and Bradypnea, and 0.99 for Tachypnea, reflecting excellent class separability, while maintaining low false positive and false negative rates. Additionally, the ROC curves lie well above the random classifier baseline, confirming reliable and robust predictions of the model across varying classification thresholds. Moreover, Figure 5c shows a class-wise confusion matrix with minimal errors, where Bradypnea, Eupnea, and Tachypnea are represented by "B", "E", and "T", respectively. This validates the effectiveness of SHAP-selected features and the model's robustness on mouth-derived data.

Figure 6 summarizes the performance of the ensemble model trained on nose-based data. As shown in Figure 6a, training accuracy stays high at around 93 % suggesting that the model fits the training data well. The CV accuracy steadily rises and converges to a mean of 85.1 %, with the final test accuracy reaching 86.7 %, indicating moderate generalization. Although a gap persists between the training and CV accuracy, the convergence trend suggests that the model benefits from increased training data and does not suffer from severe over-fitting. Moreover, the alignment of CV accuracy with test accuracy indicates reasonably good generalization. Figure 6b shows high class-wise AUCs, i.e., 0.93 for Eupnea, 0.99 for Bradypnea, and 0.92 for Tachypnea, confirming robust class separation. Moreover, all the ROC curves remain well above the random classifier baseline, demonstrating reliability and robustness of the model across varying classification thresholds. The confusion matrix in Figure 6c shows that while most misclassifications occur between Eupnea and Tachypnea, Bradypnea is identified with perfect accuracy. Overall, the model still performs reliably across all respiratory classes using nose-derived data.

7.2 Discussion

The results indicate that the ensemble model generalizes well, with no evidence of classical over-fitting. The small gap between training and CV accuracies, along with their steady alignment with test accuracy, indicates good model generalizability. This is attributed to the use of SHAP-based feature selection, the stacked ensemble approach, and class balancing with SMOTE. Classification performance is notably better for the mouth-derived data set than for the nose-derived data set, despite its smaller size. This can be explained due to the nature of airflow, as mouth breath typically results in higher exhaled volume and more distinct modulation of temperature and humidity. From an ABMC point of view, the mouth

serves as a more effective transmitter, offering a stronger encoding of information on respiratory patterns. In contrast, the nose-based model, although not hyperparameter-tuned, still demonstrates robust performance, confirming that both transmission paths carry usable features for breath pattern classification.

8 Conclusion

In this paper, we studied the possibility to identify breath abnormalities using an air-based molecular communication (ABMC) approach in combination with machine learning (ML). Our work highlights the potential of a low-cost, modest-fidelity, and non-invasive sensor for classifying human respiratory patterns. Breath patterns are treated as modulated signals from the transmitter (human) and decoded at the receiver (sensor) using ML algorithms. Despite using a simple DHT22 sensor, meaningful physiological information can be extracted from humidity and temperature signals. This approach bridges theoretical ABMC concepts with practical implementation, offering a scalable and affordable solution to continuous respiratory monitoring.

Future work will expand to include more breath patterns and integrate additional components of the communication model to develop a complete end-to-end system for health diagnostics and metabolic process detection. It will also employ more responsive sensors to improve accuracy and capture finer variations in breath biomarkers for enhanced health monitoring.

Acknowledgments

Reported research was supported in part by the project IoBNT, funded by the German Federal Ministry of Research, Technology and Space (BMFTR) under grant number 16KIS1986K, and by the project NaBoCom, funded by the German Research Foundation (DFG) under grant number DR 639/21-2.

References

[1] Ian F. Akyildiz, Massimiliano Pierobon, Sasitharan Balasubramaniam, et al. 2015. The internet of bio-nano things. *IEEE Communications Magazine* 53, 3 (March 2015), 32–40. https://doi.org/10.1109/MCOM.2015.7060516

[2] Brian A. Baldo. 2025. Opioid-induced respiratory depression: Clinical aspects and pathophysiology of the respiratory network effects. *American Journal of Physiology-Lung Cellular and Molecular Physiology* 328, 2 (Feb. 2025), L267–L289. https://doi.org/10.1152/ajplung.00314.2024

[3] Lisa Ann Baumann, Jannah Baker, Adam G. Elshaug. 2018. The impact of electronic health record systems on clinical documentation times: A systematic review. *Health Policy* 122, 8 (Aug. 2018), 827–836. https://doi.org/10.1016/j.healthpol.2018.05.014

[4] Andrew Benner, Noble F. Lewallen, Sandeep Sharma. 2023. *Physiology, carbon dioxide response curve.* StatPearls [Internet]. StatPearls Publishing. https://www.ncbi.nlm.nih.gov/books/NBK538146/

[5] Sunasheer Bhattacharjee, Dadi Bi, Pit Hofmann, et al. 2025. *Exhaled breath analysis through the lens of molecular communication: A survey.* cs.ET 2504.18326. arXiv. https://doi.org/10.48550/arXiv.2504.18326

[6] Sunasheer Bhattacharjee, Martin Damrath, Lukas Stratmann, et al. 2022. Digital communication techniques in macroscopic air-based molecular communication. *IEEE Transactions on Molecular, Biological and Multi-Scale Communications* 8, 4 (Dec. 2022), 276–291. https://doi.org/10.1109/TMBMC.2022.3220109

[7] Simon Bourcier, Maxime Coutrot, Alexis Ferré, et al. 2023. Critically ill severe hypothyroidism: A retrospective multicenter cohort study. *Annals of Intensive Care (AIC)* 13, 1 (March 2023), 1–9. https://doi.org/10.1186/s13613-023-01112-1

[8] Qiaofen Chen, Xufeng Guo, Yuyue Jiang, et al. 2023. A mobile e-nose prototype for online breath analysis. *Advanced Sensor Research* 3, 3 (April 2023), 1–9. https://doi.org/10.1002/adsr.202300018

[9] Tianqi Chen, Carlos Guestrin. 2016. XGBoost: A scalable tree boosting system. In *22nd ACM SIGKDD International Conference on Knowledge Discovery and Data Mining*. ACM, San Francisco, CA, 785–794. https://doi.org/10.1145/2939672.2939785

[10] Maximilian Christ, Nils Braun, Julius Neuffer, et al. 2018. Time series feature extraction on basis of scalable hypothesis tests (tsfresh – a python package). *Neurocomputing* 307 (Sept. 2018), 72–77. https://doi.org/10.1016/j.neucom.2018.03.067

[11] Falko Dressler, Stefan Fischer. 2015. Connecting in-body nano communication with body area networks: Challenges and opportunities of the internet of nano things. *Elsevier Nano Communication Networks* 6 (June 2015), 29–38. https://doi.org/10.1016/j.nancom.2015.01.006

[12] Raed A. Dweik, Anton Amann. 2008. Exhaled breath analysis: The new frontier in medical testing. *Journal of Breath Research (J. Breath Res.)* 2, 3 (Sept. 2008), 1–3. https://doi.org/10.1088/1752-7163/2/3/030301

[13] Ahmad Faried, Andi N. Sendjaja, Regina Melia, et al. 2016. Bradycardia without hypertension and bradypnea in acute traumatic subdural hematoma is a sensitive predictor of the Cushing triad: 3 case reports. *Interdisciplinary Neurosurgery* 6 (Dec. 2016), 84–86. https://doi.org/10.1016/j.inat.2016.10.001

[14] Nariman Farsad, Weisi Guo, Andrew W. Eckford. 2013. Tabletop molecular communication: Text messages through chemical signals. *PLoS ONE* 8, 12 (Dec. 2013), 1–13. https://doi.org/10.1371/journal.pone.0082935

[15] Alireza Ghasempour. 2024. *Support vector regression to predict power consumption.* Engineering Publications. The University of New Mexico.

[16] Maryam Khalid, Osama Amin, Sajid Ahmed, et al. 2019. Communication through breath: Aerosol transmission. *IEEE Communications Magazine* 57, 2 (Feb. 2019), 33–39. https://doi.org/10.1109/mcom.2018.1800530

[17] Amit Krishan Kumar, M. Ritam, Lina Han, et al. 2022. Deep learning for predicting respiratory rate from biosignals. *Computers in Biology and Medicine* 144 (May 2022), 1–13. https://doi.org/10.1016/j.compbiomed.2022.105338

[18] Janosch Kunczik, Kerstin Hubbermann, Lucas Mösch, et al. 2022. Breathing pattern monitoring by using remote sensors. *MDPI Sensors* 22, 22 (Nov. 2022), 1–21. https://doi.org/10.3390/s22228854

[19] Massimiliano Laddomada, Massimiliano Pierobon. 2015. A crosstalk-based linear filter in biochemical signal transduction pathways for the internet of bio-things. In *40th International Conference on Acoustics, Speech and Signal Processing (ICASSP 2015)*. IEEE, South Brisbane, Australia, 5520–5524. https://doi.org/10.1109/icassp.2015.7179027

[20] Anna Paleczek, Dominik Grochala, Artur Rydosz. 2021. Artificial breath classification using XGBoost algorithm for diabetes detection. *MDPI Sensors* 21, 12 (June 2021), 1–18. https://doi.org/10.3390/s21124187

[21] Aakash Parmar, Rakesh Katariya, Vatsal Patel. 2018. A review on random forest: An ensemble classifier. In *International Conference on Intelligent Data Communication Technologies and Internet of Things (ICICI 2018)*. Springer, Coimbatore, India, 758–763. https://doi.org/10.1007/978-3-030-03146-6_86

[22] Liudmila Prokhorenkova, Gleb Gusev, Aleksandr Vorobev, et al. 2018. CatBoost: Unbiased boosting with categorical features. In *32nd Conference on Neural Information Processing System (NeurIPS 2018)*, Samy Bengio, Hanna M. Wallach, Hugo Larochelle, Kristen Grauman, and Nicolò Cesa-Bianchi (Eds.). Curran Associates Inc., Montréal, Canada, 6639–6649. https://doi.org/10.5555/3327757.3327770

[23] Antonio Vincenzo Radogna, Pietro Aleardo Siciliano, Saverio Sabina, et al. 2020. A low-cost breath analyzer module in domiciliary non-invasive mechanical ventilation for remote COPD patient monitoring. *MDPI Sensors* 20, 3 (Jan. 2020), 1–20. https://doi.org/10.3390/s20030653

[24] Amit Sapra, Ahmad Malik, Priyanka Bhandari. 2023. *Vital sign assessment.* StatPearls [Internet]. StatPearls Publishing. https://pubmed.ncbi.nlm.nih.gov/30844173/

[25] Max Schurwanz, Peter Adam Hoeher, Sunasheer Bhattacharjee, et al. 2021. Infectious disease transmission via aerosol propagation from a molecular communication perspective: Shannon meets coronavirus. *IEEE Communications Magazine, Special Issue on Nano-Networking for Nano-, Micro- and Macro-Scale Applications* 59, 5 (May 2021), 40–46. https://doi.org/10.1109/MCOM.001.2000956

[26] Walter M. St.-John. 1998. Neurogenesis of patterns of automatic ventilatory activity. *Progress in Neurobiology* 56, 1 (Sept. 1998), 97–117. https://doi.org/10.1016/s0301-0082(98)00031-8

[27] Zhenyi Ye, Yuan Liu, Qiliang Li. 2021. Recent progress in smart electronic nose technologies enabled with machine learning methods. *MDPI Sensors* 21, 22 (Nov. 2021), 1–21. https://doi.org/10.3390/s21227620